THE EFFECT OF LOWER HYBRID CURRENT DRIVE ON THE DISCRETE ALFVEN WAVE SPECTRUM

G.A. Collins+, A.A. Howling, J.B. Lister, Ph. Marmillod

Centre de Recherches en Physique des Plasmas
Association Euratom - Confédération Suisse
Ecole Polytechnique Fédérale de Lausanne
21, av. des Bains - 1007 Lausanne/Switzerland

C. Gormezano*, F. Parlange°, J.-C. Vallet°, D. Van Houtte°

Association Euratom-C.E.A., Département de Recherches
sur la Fusion Contrôlée, C.E.N.G., Grenoble, France

Abstract - The frequencies of driven global eigenmodes of the Alfvén wave have been measured on the PETULA tokamak during experiments on Lower Hybrid Wave Current Drive (LHCD). Small but significant and reproducible shifts in their resonant frequencies were measured, which varied depending on the LHCD rf power. Explanations for these frequency changes are discussed.

+present address : A.A.E.C., Australia

*present address : JET, Abingdon, U.K.

°present address : Association Euratom-C.E.A., C.E.N., Cadarache, France

Lower Hybrid current drive (LHCD) experiments carried out on the PETULA tokamak (R,a = 0.71, 0.17m, B_{ϕ} ~ 2.8T) have demonstrated the suppression of the sawtooth instability under certain conditions (VAN HOUTTE et al. 1984, and PARLANGE et al. 1986). It is not yet totally clear to what extent the sawtooth suppression can be attributed to a change in the current profile which would allow q(0) to increase above unity, or to some direct stabilisation mechanism. Suppression of the sawtooth activity has subsequently also been reported by other experiments, reviewed by GORMEZANO (1986).

This question as to the origin of the stabilisation motivated a detailed study on the use of the resonant frequencies of global eigenmodes of the Alfvén Wave, known as Discrete Alfvén Waves (DAW), to detect variations in the central value of the safety factor, q(0), during the LHCD rf pulse. This study by COLLINS et al. (1986) showed that the measurement of the DAW spectrum and the tracking of one resonance, using a single simple antenna, was technically feasible, even at low rf probing power. However, their analysis showed that the DAW spectrum cannot yield an unambiguous value of q(0) if the form of the current profile is not specified. It was demonstrated that the spectrum is more generally sensitive to an overall peakedness of the current profile, for example to a simple global parameter such as the internal inductance, li. Although the absolute measurement of q(0) was not possible, the results obtained during the LHCD experiments on PETULA do nevertheless contain interesting information on the phenomena occuring when current is driven by the rf, and those results have motivated this present letter. In what follows, we shall only very briefly describe the experimental arrangement and the theoretical background to the DAW spectrum. The results are then presented and their significance discussed.

The experimental layout, described in detail by COLLINS et al. (1986), consists of a single antenna launching about 10 Watts in the frequency range 2 - 8 MHz. Synchronous detection of the driven eigenmodes uses a single multi-turn coil oriented so as to pick up the toroidal component of the fluctuating magnetic field. Using a phase-sensitive feedback system it was possible to track the frequency of the DAW as the plasma conditions evolved. The time resolution was sufficient to detect the modulation of the DAW resonant frequency by the sawtooth relaxations.

The resonant frequency, ω_{DAW} of an eigenmode labelled (n,m) is close to the threshold frequency, ω_{min}, of the Shear Alfvén Wave (SAW) continuum of that mode, expressed in the cylindrical approximation by

$$\omega_{DAW} < \omega_{min} < \omega_A(0) = (n+m/q(0)) \cdot B_\phi \cdot (1-\omega_A{}^2/\omega_{ci}{}^2)^{1/2} \cdot (\mu_0 \rho(0) R_0{}^2)^{-1/2} \quad (1)$$

in which (n,m) are the toroidal and poloidal mode numbers respectively and $q(0)$, $\rho(0)$ and $\omega_A(0)$ are the safety factor, mass density and SAW frequency on axis respectively. Equation (1) suggests that the values of ω_{DAW} will be very sensitive to $q(0)$. However the difference between ω_{DAW} and $\omega_A(0)$ also depends sensitively on $\rho(r)$ and $q(r)$, so that it can no longer be assumed that ω_{DAW} is as closely related to $\omega_A(0)$ as had been hoped. This is due to the global nature of the eigenmode of the Alfvén wave. When $\rho(r)/\rho(0)$ and $j(r)$ are fixed, numerical calculations of the resonance frequency show that the dependence of the frequency on the central mass is given by

$$\omega_{DAW} \sim \rho(0)^{-0.45} \qquad (2)$$

for all (n,m). This separability of the absolute value of density is important for the evaluation of the results, and is true for $\omega \ll \omega_{ci}$. In toroidal geometry we must also be prudent regarding the values of B_ϕ and R_0, since the resonance condition has not been studied numerically during changes in the non-concentricity of the magnetic surfaces as may occur in toroidal geometry. All the experiments carried out in PETULA used deuterium as the filling gas, and so the variation in the effective ion mass per electron, due to any changes in impurity content, is assumed to be negligible.

We can therefore summarize the interpretation of any change in the frequency of a DAW as a mixture of the following :

(i) $\rho(r)/\rho(0)$ is changing,

(ii) $\rho(r)/\rho(0)$ is fixed but $\rho(0)$ is changing,

(iii) $j(r)$ is changing.

We now turn to the experimental results. The Lower Hybrid waves are launched in PETULA at a frequency of 3.7 GHz from a multijunction waveguide grill, so as to drive a wave parallel to the electron drift direction. The spectrum of Lower Hybrid waves launched is centred around $n_\parallel$ = 1.7. This high frequency has allowed current drive experiments to be carried out at densities up to $8 \cdot 10^{19} m^{-3}$ with suppression of the sawtooth instability studied up to $\bar{n}_e = 6.5 \times 10^{19} m^{-3}$. Figure 1 shows characteristic traces during a

PETULA discharge with $\bar{n}_e = 3.2 \cdot 10^{19}$ and a 30msec, 200kW rf pulse. The loop voltage decreases slowly under feedback control at constant plasma current, reaching a minimum after ~20msec. The signal from a centrally-viewing soft X-ray detector shows that the sawtooth relaxation is stabilised immediately after the start of the rf pulse, within one sawtooth period. The central soft X-ray emission increases by more than a factor of 2, and then drops during an increase in $m = 1$ oscillations seen on the soft X-ray signals. The emission profile is measured to be peaked for the first 10ms and relaxes to a broad profile, broader than the ohmic one. The upper trace shows the time-varying frequency of the low-power probing generator as it tracks the $(n,m) = (-2,-1)$ DAW. The noise level in this signal must be less than the thickness of the frequency trace, and is far less than the major changes observed. The shot-to-shot reproducibility is better than this noise level. During the LHCD pulse, the DAW frequency drops abruptly and its variation follows several distinct phases.

Figure 2 further illustrates these changes,with results for a series of different DAWs with $(n,m) = (-1,-1)$ through to $(-4,-1)$. The variations in the frequencies of all these modes show the same gross behaviour, indicating that a large part of the change may be due to a density increase (Equation (2)). The fact that the modes do, however, show a different behaviour in detail suggests that the profiles must also be changing at the same time, since the different resonances have different sensitivities to changes in $j(r)$ and $\rho(r)$.

Two sequences of discharges were performed with increasing LHCD rf power delivered to the plasma, and with the delivered LHCD power constant during the rf pulse. In the first series, Fig. 3a), total suppression of the sawteeth was obtained for injected power P > 98kW, seen on the $\emptyset_X$ trace. For the second series, Fig. 3b), a carbon guard limiter was introduced close to the grill and although the sawtooth activity was deeply modified, it was not totally suppressed even with 184kW launched. The difference was presumed to be due to the change in the edge plasma at the grill mouth which either changed the effective rf power delivered, or the effective spectrum launched. In fact the X-ray emission behaviour was similar for both series if shots are compared at equal loop voltage drop rather than equal launched power, indicative of a loss of global efficiency.

Figure 3b) shows a most remarkable correlation between the change in the DAW frequency and the change in soft X-ray emissivity. This similarity between the signals was maintained as the power level increased, and they even mirrored each other in minor details. In the other series, Fig. 3a), this precise mirroring was absent, with the DAW frequency reacting much more rapidly than the soft X-ray signal on application of the rf pulse. The evolution of the highest power shot shows the separate phases of the evolution most clearly (Fig. 1). First the DAW frequency dropped. Then it remained almost stationary while the soft X-ray flux increased. Then the soft X-ray flux dropped, during increased m = 1 activity, and the DAW frequency increased. A quasi-stationary state was then reached with the sawteeth suppressed. Finally, when the rf pulse was turned off, the sawtoothing activity returned immediately, and there was a large positive excursion of the

DAW frequency. The sawtooth activity is also seen on the DAW frequency in this figure, most strikingly during the large sawteeth seen after the end of the rf pulse. This modulation can be due to the density or current profile modulation or, of course, both (de CHAMBRIER et al. (1982)).

There is generally a small increase in the central line-integrated electron density during the rf pulse. The resolution of the interferometer ($7.5 \cdot 10^{11}cm^{-3}$) is insufficient to determine whether the temporal evolution of this change is identical to that of the DAW frequency. In the 193kW shot of Fig. 1, one of the first series of Fig. 3a), the drop in the DAW frequency is -40.3kHz, 0.99% of the initial value. This would be caused by a density increase of 2.2% over the whole density profile (Eq. (2)) and the measured increase in n_e is ~3.2%, clearly of the same order. However, the rise in n_e occurs appreciably later than the drop in the DAW frequency. This could, in principle, be due to an initial rapid peaking of the density profile, although none of the interferometric measurements would support this, and such a peaking could not even conserve the number of particles in the plasma. The similarity between the soft X-ray and DAW frequency signals in Fig. 3b) must also be explained. Whereas the DAW frequency change would correspond to a few percent change in $n_e(0)$, the observed 140% increase in the soft X-ray flux certainly would not. However, their remarkable similarity forces us to expect a causal connection between the two signals. Since the evolution of the density cannot fully explain the evolution of the DAW frequency in the series with efficient sawtooth suppression, the initial rapid drop in frequency as well as the rapid relaxation overshoot already remarked on, remain to be explained. Such an effect could be produced by an initial drop in j(0), as can be seen from Equation (1) in which the $q(r\sim0)$ dependence resembles mj(0). This would then make the presence of the m = 1 oscillations difficult to understand if q(0) were brought above 1. Subsequently a rapid increase in j(0) would follow the end of the rf pulse. As pointed out already, the DAW frequency varies with li rather than q(0) when the current profile form is varied. The flattening and peaking in the current profile does not then imply that the value on axis is changing. A change of -1% in the DAW frequency would correspond to a decrease in li of 0.06 (COLLINS et al., (1986)), when the sawteeth are suppressed, even when q(0) is held fixed.

The increase in the soft X-ray flux cannot be due to an increase in the density (56% increase needed) nor to an increase in the electron bulk temperature (34% increase needed, if $\emptyset_X \sim T_e^3$). A large increase in Te(0) is not observed. We must therefore conclude that this increase is due to the fast electron population (30 - 200keV) driven by the rf wave. The increased X-ray flux would then be due to "free-bound" interactions with impurity ions already present in the plasma, but this has not been experimentally confirmed on PETULA. It is then plausible that the small change in li inferred might be simply due to the radial distribution of the fast electron current. At low density it seems clear that the particle confinement time increases during rf injection because the rise in n_e coincides with a decrease in density beyond the limiter and a fall in H_β radiation. The density change, then, might be due to an influx of particles during the rf pulse, although we must not exclude the possibility that a change in the plasma current profile might also lead directly to a change in the plasma density profile.

To summarize, we have shown that the frequency of the Alfvén Wave global eigenmodes shifts systematically during the LHCD pulse on PETULA. Part of this shift may be due to a change in the central mass density but some of the shift must be due to a change in the current profile, corresponding to a small decrease in the internal inductance. The shift in frequency has a different temporal evolution for the cases when the sawtooth activity is, or is not, efficiently suppressed. This strongly suggests that the suppression depends on a flattening of the current profile. On the other hand, the constancy of the sawtooth inversion radius for powers up to the threshold for sawtooth suppression and the existence of the m=1 mode means that this change in current profile leads to $q \sim 1$ in a large central zone, or eventually to a non-monotonic q profile. Although the DAW spectrum cannot yield an unambiguous value of q(0), or even $\Delta q(0)$, this diagnostic has indicated the presence of extremely reproducible and temporally highly structured changes in the plasma parameters, undetected by the other measurements available, which must be explained.

Acknowledgements - We are grateful for the support of Dr. G. Briffod and Prof. F. Troyon in encouraging this collaboration. This work was partly supported by the Fonds National Suisse de la Recherche Scientifique.

REFERENCES

de CHAMBRIER, A., DUPERREX, P.A., HEYM, A., HOFMANN, F., JOYE, B., KELLER, R., LIETTI, A., LISTER, J.B., POCHELON, A., SIMM, W., Phys. Letts. 92A, 279 (1982)

COLLINS, G.A., HOWLING, A.A., LISTER, J.B., MARMILLOD, Ph., Plasma Phys. and Contr. Fus., in press (1986), LRP 294/86

GORMEZANO, C., Plasma Phys. and Contr. Fus., 28, 1365 (1986)

PARLANGE, F., BRIFFOD, G., GIRARD, A., GORMEZANO, C., HOANG, G.T., RAX, J.M., VAN HOUTTE, D., XI Int. Conf. Plasma Physics and Contr. Fusion, F-II-3, Kyoto (1986)

VAN HOUTTE, D., BRIFFOD, G., CHABERT, P., GORMEZANO, C., HOW, J., ICHTCHENKO, G., MELIN G., MOULIN, B., PARLANGE, F., VALLET, J.-C., Nucl. Fus. 24, 1485 (1984)

FIGURE CAPTIONS

Fig. 1 - Typical traces during a PETULA discharge. The LHCD rf pulse (~193kW) is applied for 30msec at t = 150msec [I_p=120kA, D_2]. The evolution of the (n,m) = (-2,-1) eigenfrequency is shown.

Fig. 2 - The evolution of the DAW frequency for several eigenmodes. [I_p=120kA, D_2]

Fig. 3 - Sequences of shots with different rf powers, showing the variation in the (n,m) = (-2,-1) DAW frequency and the intensity of the X-ray emission along a central chord with (a) full suppression of sawteeth and (b) only partial suppression of sawteeth [I_p=120kA, D_2]. Both series had the same target density, $\bar{n}_e = 3.2 \times 10^{19} m^{-3}$.

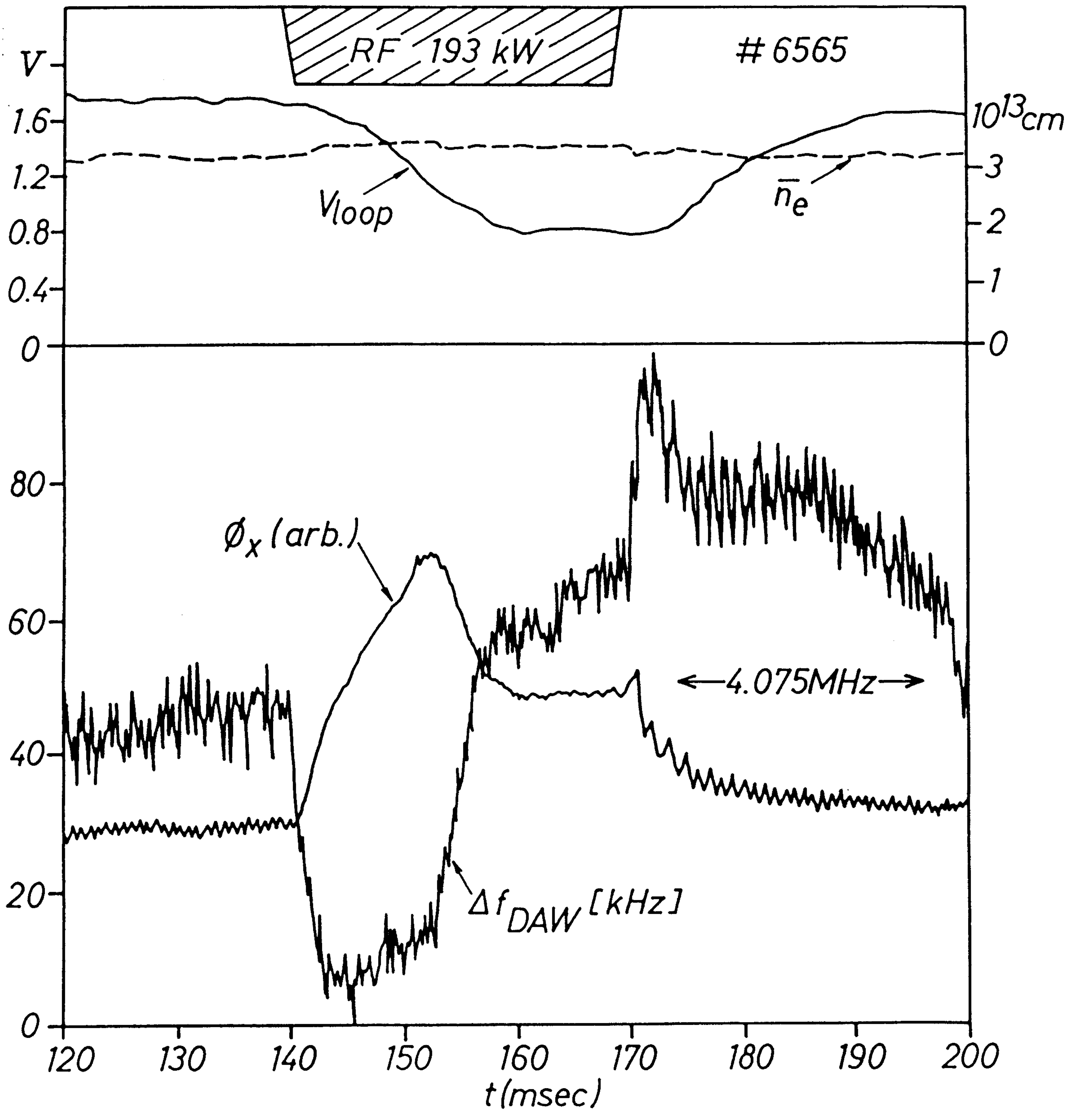

RF 193 kW
6565
V
1.6
1.2
0.8
0.4
0
10^{13}cm
3
2
1
0
V_{loop}
$\bar{n}_e$
80
60
40
20
0
ϕ_x (arb.)
Δf_{DAW} [kHz]
4.075MHz
120
130
140
150
160
170
180
190
200
t (msec)

Fig. 1

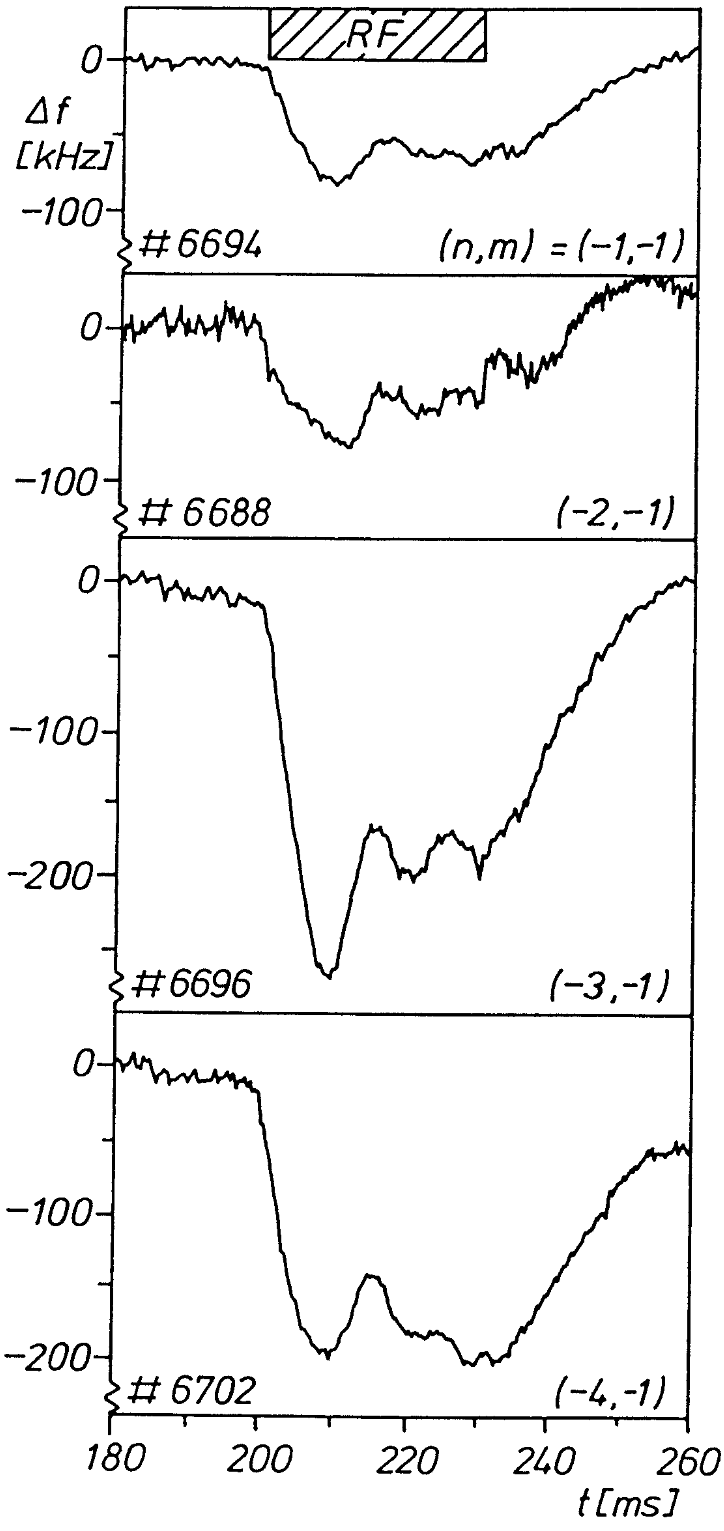
RF
0
Δf
[kHz]
-100
6694
(n,m) = (-1,-1)
0
-100
6688
(-2,-1)
0
-100
-200
6696
(-3,-1)
0
-100
-200
6702
(-4,-1)
180
200
220
240
260
t[ms]

Fig. 2

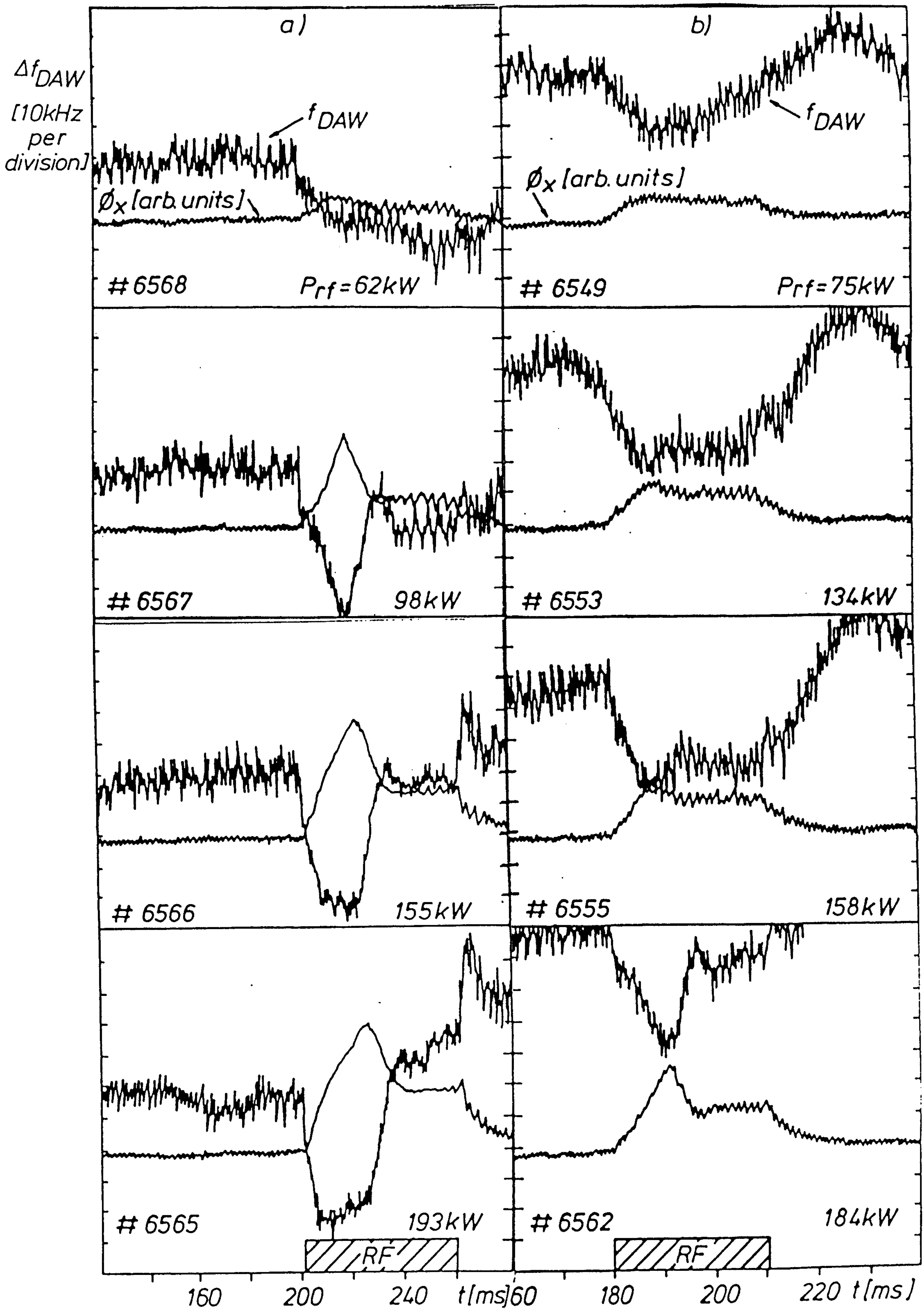

a)
b)
Δf_{DAW}
[10kHz per division]
f_{DAW}
$\emptyset_x$ [arb. units]
6568
P_{rf} = 62kW
6549
P_{rf} = 75kW
6567
98kW
6553
134kW
6566
155kW
6555
158kW
6565
193kW
6562
184kW
RF
160
200
240
t [ms]
160
180
200
220
t [ms]

Fig. 3